Mechanistic Description of Photochemical Oligomer Formation from Aqueous Pyruvic Acid

Rebecca J. Rapf,[†] Russell J. Perkins,[†] Barry K. Carpenter,[‡] and Veronica Vaida*,[†]

[†]Department of Chemistry and Biochemistry and Cooperative Institute for Research in Environmental Sciences, University of Colorado Boulder, Boulder, Colorado 80309, United States

[‡]School of Chemistry and the Physical Organic Chemistry Centre, Cardiff University, Cardiff CF10 3AT, United Kingdom

* Supporting Information

ABSTRACT: The aqueous phase photochemistry of pyruvic acid, an important oxidation product of isoprene, is known to generate larger oligomeric species that may contribute to the formation of secondary organic aerosol in the atmosphere. Using high resolution negative mode electrospray ionization mass spectrometry, the aqueous photochemistry of dilute solutions of pyruvic acid (10, 1, and 0.5 mM) under anaerobic conditions was investigated. Even at the lowest concentration, covalently bonded dimers and trimers of pyruvic acid were observed as photochemical products. We calculate that it is energetically possible to photochemically generate parapyruvic acid, a dimer of pyruvic acid that is known to form via dark oligomerization processes. Subsequent photochemical reactions of parapyruvic acid with pyruvic acid form larger oligomeric products, such as 2,4-dihydroxy-2-methyl-5-oxohexanoic acid. A robust and relatively simple photochemical mechanism is discussed that explains both the conditional dependence and wide array of products that are observed.

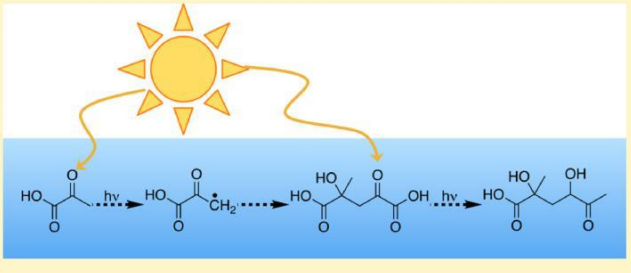

INTRODUCTION

Atmospheric aerosols are known to contribute to pollution-related smog and haze, affecting visibility and human health;[1,2] in addition, they have considerable influence over the global radiative budget.[3−10] The impact of atmospheric aerosols on radiative forcing is currently the largest source of uncertainty in climate models, with significant contributions to the accumu-lated error occurring from the effort to quantify secondary organic aerosol (SOA).[11] SOA, particles generated in the atmosphere through the oxidation of volatile organic compounds (VOCs), are the major contributor to aerosol mass in remote areas.[8,12,13] Recent work suggests that oligomers formed from aqueous phase photochemistry of small organics may contribute significantly to the formation and development of SOA.[8,9,14−22] Therefore, the generation of such molecular complexity via multiphase chemistry is critical in the understanding of the formation of SOA.

The chemistry governing the formation of SOA from small organics is inherently complex, involving interwoven networks of reactions between many species. As we show, even a single, simple three-carbon molecule can yield a surprisingly rich chemistry. Here we examine the aqueous phase photochemistry of a model species, pyruvic acid, under acidic, anaerobic conditions, suggesting a new identification and mechanistic pathway for observed oligomeric species. By developing mechanistically the potential reactive pathways for aqueous pyruvic acid, we may add to the understanding of its possible photochemical fates in the natural environment.

Pyruvic acid, a key oxidation product of isoprene in the environment,[23−25] is found in both the gas and aqueous phases in the atmosphere.[23,26−34] The simplest of the α-keto acids, pyruvic acid has also been used as a proxy for atmospheric α-dicarbonyls.[24,25,28,35] Pyruvic acid absorbs light in the near-UV from the solar photon flux reaching the surface of the Earth and is oxidized relatively slowly by H_2O_2 and the hydroxyl radical (OH).[36−40] Consequently, the main atmospheric sink for pyruvic acid is direct photolysis; in the aqueous phase, this photochemistry has been linked to oligomer formation and the production of SOA.[21,37,41−45]

While a seemingly simple, three-carbon molecule, pyruvic acid's reactivity is extremely diverse and dependent on reaction conditions. Its chemistry spans a wide variety of processes and environmental conditions, including gas and aqueous photo-chemistry,[37,42−60] multiphase photochemistry,[61] oxidation by H_2O_2 and hydroxyl radicals,[25,36,38−40] thermal decomposi-tion,[62−64] and multiphoton pyrolysis.[65] Pyruvic acid is also known to spontaneously oligomerize in aqueous solution or as a pure liquid, even in the dark, forming a variety dimer species that include zymonic acid and parapyruvic acid.[66]

The photochemical pathways available to pyruvic acid are strongly phase dependent. In the gas phase, absorption of a UV photon (λ_{max} ~ 350 nm) promotes ground state pyruvic acid to the first excited singlet state (S_1, $^1(n, \pi^*)$), whereupon it

decomposes, forming CO_2 and acetaldehyde, with additional minor products.[36,48,54,55,57−59,67,68] However, the species produced by this gas phase photochemistry can be affected by changing the buffer gas, total pressure, and composition.[58] Different photochemical pathways become accessible in the aqueous phase than in gas phase[41,43−45,56,60] because interactions with water affect pyruvic acid's electronic structure, changing its photophysical and photochemical mechanisms.

The λ_{max} of the S_1, $^1(n, \pi^*)$, state shifts to the blue ($\lambda_{max} \sim 320$ nm) such that, following excitation, intersystem crossing and internal conversion to the T_1, $^3(n, \pi^*)$ state occurs, subsequently generating organic radicals. These radicals then react further, often recombining to generate oligomeric species.

Recent work on the aqueous photochemistry of pyruvic acid has exposed its extreme sensitivity to the environment: the rate of decomposition and resulting products are dependent on both the concentration of pyruvic acid and on the atmospheric composition.[37,61] This sensitivity to reaction conditions likely explains some of the discrepancies in the literature about some minor photoproducts;[37,41−45,69,70] however, there is broad agreement that the major aqueous photochemical pathways generate more complex oligomeric species,[37,42,43] including covalently bonded dimers and trimers[71] of pyruvic acid. In this work, we structurally characterize oligomeric species and propose a new mechanistic pathway by which these oligomers are photochemically formed through reactions with reactive intermediate species.

EXPERIMENTAL SECTION

Pyruvic acid (98%, Sigma-Aldrich) was distilled twice under reduced pressure (<1 Torr) while heating gently (<55 °C) and diluted with 18.2 MΩ water (3 ppb TOC) to make solutions of 10, 1, and 0.5 mM concentration. For each 100 mL volume solution, 10 mL of the solution was saved as a pre-irradiation control, and the remaining 90 mL of solution were illuminated for 5 h in a temperature-stabilized water bath at 4 °C with a 450 W Xe arc lamp (Newport). The lower concentration solutions (1 mM and 0.5 mM) were also irradiated with the water bath held at 20 °C. There was no difference in observed products based on water bath temperature. Unless otherwise specified, all solutions were purged with N_2 to displace dissolved O_2, beginning 1 h prior to the start of irradiation and continuing for the duration of the experiment. Oxygen-depleted conditions are known to favor formation of the oligomeric species under study here,[37] allowing for easier analysis and identification of products at relatively low reaction concentrations. The irradiated solutions were allowed to come to room temperature before any further analysis was conducted.

The solutions were used without adjustment from their natural pH, meaning all photochemical experiments were conducted under acidic conditions. There is a slight variance in the pH of the solutions as a function of the concentration of pyruvic acid, increasing with decreasing concentration. The pH of the 10 mM pyruvic acid solutions was ~2.4 and rises to approximately 3.5 for the 0.5 mM pre-irradiation solutions.

The Xe arc lamp used was not filtered, meaning that its output extends into the UV to about 220 nm as shown in the Supporting Information, Figure S1. Because of the extended light in the UV, under our experimental conditions, it is likely some excitation to the S_2, $^1(\pi, \pi^*)$, state in addition to the S_1 state also occurs. However, as is common with excitation to higher excited states,[72,73] it is likely that the system in the S_2 rapidly undergoes internal conversion to the lower S_1 state before following the same photochemical pathway of intersystem crossing and internal conversion to the reactive T_1 state. The photochemical products observed here using with the unfiltered Xe arc lamp are in good agreement with the previous results generated with a filtered Xe arc lamp with wavelengths $\lambda < 300$ nm removed from the spectrum.[37] In the latter case, the radiation provided can excite the S_1 but not the S_2 state, suggesting the same reactive photochemical pathway is preserved. The rate of photochemistry is, however, increased when the light is not filtered, as would be expected when more photons are present. These observations are consistent with those in the literature, which have shown, for example, that the photochemistry of nonanoic acid in aqueous solution using a filtered Xe arc lamp is observed to slow but not result in significantly different products than when not filtered.[74]

Electronic Structure Calculations. Calculations with the composite CBS-QB3 model[75] and using the Gaussian 09 suite of programs[76] were conducted on the relative barriers to H atom abstraction from the methyl and carboxyl groups of pyruvic acid S_0 by pyruvic acid T_1, $^3(n, \pi^*)$. The calculations suggested that the activation enthalpy for the former is only 1.47 kcal/mol greater than that for the latter. Details are provided in the Supporting Information.

UV−Vis Spectroscopy. Pre- and post-irradiation solutions of the oxoacids were scanned using a Varian (Agilent) Cary 5000 spectrometer with a 0.1 s average time, 0.5 nm data interval, and a 0.5 nm spectral bandwidth.

NMR Analysis. NMR experiments were obtained at 23 °C using a Varian INOVA-500 NMR spectrometer operating at 499.60 MHz for ^1H detection. To perform experiments in aqueous solution, an optimized WET solvent suppression pulse sequence was used to eliminate >99% of the H_2O signal.[77]

Mass Spectrometry Analysis. High resolution mass spectrometry was performed on a Waters Synapt G2 HDMS mass spectrometer using electrospray ionization operated in negative mode. Instrument parameters remained constant and were as follows: analyzer, resolution mode; capillary voltage, 1.5 kV; source temperature, 80 °C; sampling cone, 30 V; extraction cone, 5 V; source gas flow, 0.00 mL/min; desolvation temperature, 150 °C; cone gas flow, 0.0 L/h; desolvation gas flow, 500.0 L/h.

Instrument parameters were chosen to minimize the potential for in-source fragmentation and reactions due to ionization. Under the ionization conditions used here, we observe both $[M - H]^-$ and singly charged adduct ions for the analytes of interest. The adducts identified are formed from two or more deprotonated organic species coordinated to a metal ion, yielding a noncovalent adduct ion with a net charge of −1. In the pyruvic acid solutions, especially before irradiation, we observe adduct ions consisting of multiple deprotonated pyruvic acid molecules coordinated with a positive counterion, usually Na^+ or Ca^{2+} at quite high intensities, as shown in the Supporting Information, Table S1 and Figure S2. To minimize the presence of adduct ions, all photochemical experiments were conducted in 18.2 MΩ water without the addition of salt, and any such metal ions are assumed to be only present in trace quantities.

The ESI^- mass spectrometry analysis conducted here is not designed to be absolutely quantitative. As expected, we observe $[M - H]^-$ ions for a number of species with observed intensities varying considerably due to variations in ionization efficiency for these analyte mixtures. We applied a conservative intensity threshold of 10^4 counts for analyte identification to

Table 1. Select Compiled Pyruvic Acid Photochemistry ESI$^-$ MS Data[a]

assigned formula $[M-H]^-$	assigned structure	average experimental m/z[b]	theoretical m/z	mass diff (ppm)	pre-irradiation	post-irradiation
		Pre-irradiation Species				
$C_3H_3O_3$	pyruvic acid	87.0091 ± 0.0005	87.0082	10.8	strong	strong
$C_3H_5O_4$	2,2-dihydroxypropanoic acid (Pyruvic diol)	105.0190 ± 0.0007	105.0188	2.3	weak	below threshold
$C_6H_7O_6$	parapyruvic acid[c]	175.0243 ± 0.0004	175.0243	0.21	weak	below threshold
		Key Photochemical Products				
$C_4H_7O_2$	acetoin	87.0454 ± 0.0007	87.0446	8.7	below threshold	medium
$C_3H_5O_3$	lactic acid	89.0239 ± 0.0003	89.0239	0.45	below threshold	weak
$C_5H_7O_4$	acetolactic acid	131.0354 ± 0.001	131.0345	6.6	below threshold	medium
$C_7H_{11}O_5$	DMOHA[d]	175.0617 ± 0.0006	175.0607	5.5	below threshold	strong
$C_6H_9O_6$	dimethyltartaric acid	177.0409 ± 0.0005	177.0400	5.0	below threshold	strong
$C_8H_{11}O_7$	CDMOHA[e]	219.0512 ± 0.0009	219.0505	3.2	below threshold	medium

[a]Chemical formulas are assigned as the ionized $[M-H]^-$ species, structures are assigned as the neutral species. [b]The experimental m/z is the observed average across experiments, and the uncertainty given is the 95% confidence interval. [c]The peak assigned to parapyruvic acid likely also has contributions from the closed ring form of zymonic acid diol as well. [d]DMOHA = 2,4-dihydroxy-2-methyl-5-oxohexanoic acid [e]CDMOHA = 4-carboxy-2,4-dihydroxy-2-methyl-5-oxohexanoic acid

avoid incorrect ion assignments to noise peaks; the noise threshold is about 1000 counts. For comparative purposes, categories of signal intensity are defined as follows: "strong" ions display intensities greater than 10^6 counts, "medium" ions display intensities greater than 10^5 counts, and "weak" ions display intensities greater that 10^4 counts for the monoisotopic ion in all cases. It is important to note that these intensity categories do not necessarily correlate directly to absolute analyte concentrations and are used for relative comparisons only.

RESULTS AND DISCUSSION

The aqueous chemistry of pyruvic acid is generally defined by the formation of oligomeric species, under both light and dark conditions. The aqueous phase photochemistry of pyruvic acid has been studied previously in the literature[41,43−45,56,60,61] and is known to generate a surprisingly complex mixture of observed photoproducts, many of which have been assigned following the literature mechanism.[37,43] Here, studying the aqueous phase photochemistry of pyruvic acid with high-resolution negative mode electrospray ionization mass spec-trometry (ESI$^-$ MS), we are able to suggest a new structural identification for oligomeric photoproducts. The new mecha-nistic pathway we suggest for these products is informed by a recent investigation of the dark oligomerization processes of pyruvic acid,[66] as well as recent results examining the multiphase photochemistry of pyruvic acid in an environmental simulation chamber.[61]

Pre-Irradiation Solutions and Dark Processes. The generation of covalently bonded dimers of pyruvic acid in the dark has been known since the 19th century;[78−80] nevertheless, these dark processes have been largely ignored by the modern literature. Recently, however, it has been demonstrated that pyruvic acid, either pure or in aqueous solution, will spontaneously dimerize, likely through an aldol addition reaction.[66] The dimerization products include parapyruvic acid and zymonic acid, the lactone enol form of parapyruvic acid (see Scheme 2 for structures). In aqueous solution, there is an equilibrium between pyruvic acid, parapyruvic acid, zymonic acid, and their tautomers and hydrates, which depends on the concentration and pH of the solution.[66]

When studying the photochemical products generated by pyruvic acid, it is necessary to consider whether the oligomerization processes that take place in the dark may be contributing to the identified products. However, such dark oligomerization processes do not occur on a time scale that competes with the observed photochemistry. As observed in the MS data, the rate of formation of these dimerization products in pure, distilled pyruvic acid stored 4 °C occurs over the course of weeks. As shown by NMR analysis in the Supporting Information, Figure S3, there is very little contamination present in the 10 mM aqueous solutions before irradiation, with conservative estimates placing an upper limit on zymonic acid of <0.1%. As mentioned above, the equilibrium between pyruvic acid and the various forms of parapyruvic and zymonic acid shifts as a function of concentration. In the dilute aqueous solutions under which photochemistry was conducted here, the equilibrium favors the reformation of monomeric pyruvic acid from dimerization products that may have been formed in the pure pyruvic acid. The kinetics of this shift are slow, but they provide reassurance that further dark dimerization products are not formed quickly enough to influence either the light-initiated chemistry or analysis in these experiments.

Although the overall concentration of the pyruvic acid dimers formed by dark reactions is low in our pre-irradiation samples, the presence of zymonic acid species is detectable by our ESI$^-$ MS analysis. There are six species derived from zymonic acid, including parapyruvic acid, that exist in aqueous solution.[66] Because these are closely related tautomers and enols, the chemical formulas of these species overlap. For example, using ESI$^-$ MS we detect an ion with an average experimental m/z for $[M-H]^-$ of 175.0239, which suggests the molecular formula $C_6H_8O_6$. This likely represents both parapyruvic acid and the closed ring form of the zymonic acid diol. Of the equilibrium species of zymonic acid in aqueous solution, these structures are the favored species.[66] In our analysis of the MS data (see Table 1 and Supporting Information, Table S1), we applied a conservative intensity threshold of 10^4 counts for analyte identifications to avoid incorrect ion assignments to noise peaks (see Experimental Section for more detail). The ions that correspond to parapyruvic acid and the closed zymonic diol are consistently observed above this threshold for the 10 mM pyruvic acid solutions before irradiation. Ions corresponding to the other zymonic acid species were observed occasionally at this threshold of intensity but were not consistently observed

Scheme 1. Aqueous Photochemical Pathways for Pyruvic Acid.[37,43]

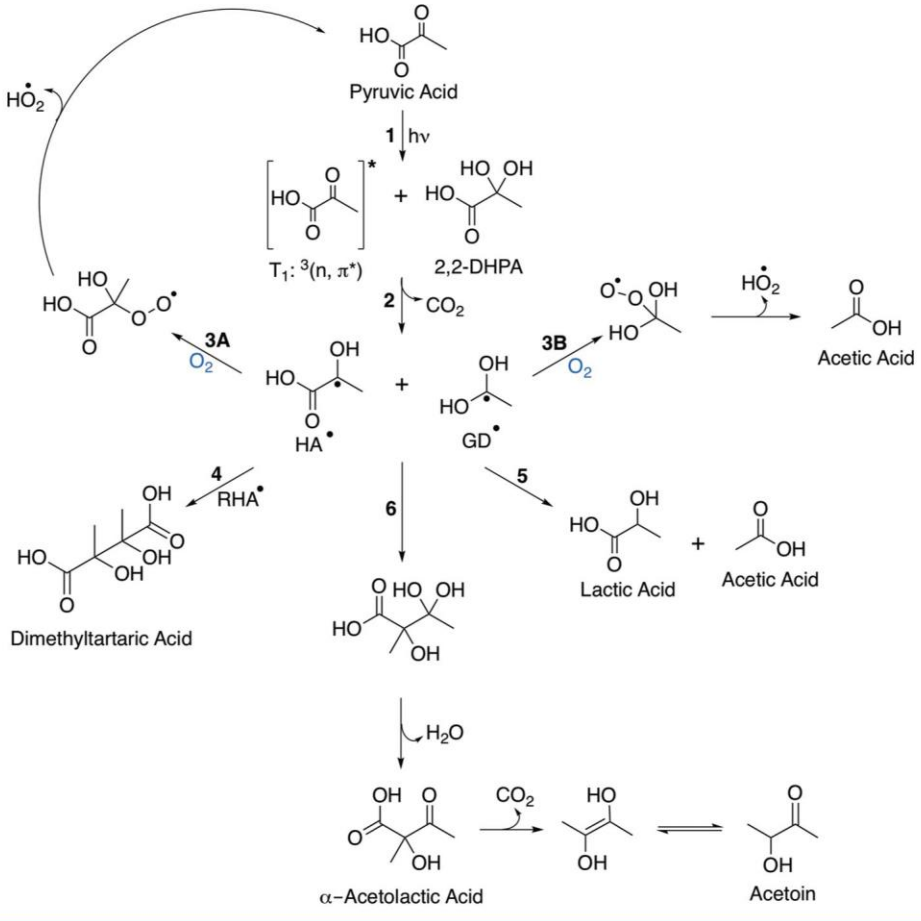

above the intensity cutoff we implemented. At the lower pyruvic acid solution concentrations (e.g., 1 and 0.5 mM), ions from zymonic acid are not generally observed in the mass spectra above the threshold. It is not surprising that the presence of zymonic acid is not observable at low concentrations of pyruvic acid; an already very low concentration of the contaminant is spread over multiple equilibrium structures, making it less likely that it would rise above our conservative threshold for detection.

Parapyruvic acid and other zymonic acid derivatives are not generally observed in the post-irradiation solutions with intensities that rise above our threshold for detection. The lack of signal from parapyruvic acid in the ESI^- MS of post-irradiation solutions suggests that most of it has been consumed during the photochemical experiments. This is not surprising because parapyruvic acid is itself an α-keto acid and therefore photoactive. Similarly, if any parapyruvic acid was generated photochemically during the course of irradiation, it may not be detected in the post-irradiation samples. This raises the possibility that these species might also be synthesized photochemically and act as reactive oligomeric intermediate species whose further chemistry contributes to the observed photoproducts in the light-initiated chemistry of pyruvic acid, as is discussed in detail below. The recent observation of zymonic acid as a photoproduct generated from the irradiation of multiphase pyruvic acid under atmospherically relevant conditions in environmental simulation chamber studies[61] lends credence to the photochemical formation and subsequent photochemistry of parapyruvic acid that may take place in aqueous solution.

Photochemical Oligomerization Processes. As men-tioned above, photochemistry in aqueous solution begins upon absorption of a photon by the α-keto acid in the near UV. The absorption maximum of this transition occurs for pyruvic acid at a wavelength of ~320 nm (Supporting Information, Figure S1). In aqueous solution, the ketone group of pyruvic acid can be hydrated to form a geminal diol, 2,2,dihydroxypropanoic acid, (2,2-DHPA).[81−84] Unlike the ketone form, the geminal diol conformer does not absorb light within the solar spectrum. Many α-dicarbonyl species undergo almost complete hydration to the diol form in aqueous solution, where catalysis by water, acid, or base lowers the relatively high reaction barriers.[85−87] Pyruvic acid retains significant amounts of the ketonic functionality. The extent of hydration is both pH- and temperature-dependent,[82,88] but at 298 K, aqueous pyruvic acid generally exists as ~40% in the keto and ~60% in the diol form.[37,42,83,84] However, this ratio is concentration dependent as well. For the 10 mM solutions of pyruvic acid investigated here, the ratio is closer to 50% keto and 50% diol (Supporting Information, Figure S3). This ratio shifts during the photo-chemical experiments to slightly favor the keto form, which is likely due to the coupled effects of the depletion of pyruvic acid and subsequent slight decrease in acidity of the solution. All photochemical experiments were conducted without adjusting the solutions from their natural pH. The pH of the solution is increased slightly as the concentration of pyruvic acid is lowered. For the 0.5 mM pre-irradiation solutions, the pH is

Scheme 2. Photochemical Generation of Parapyruvic Acid via Hydrogen Abstraction from the Methyl Group of Pyruvic Acid

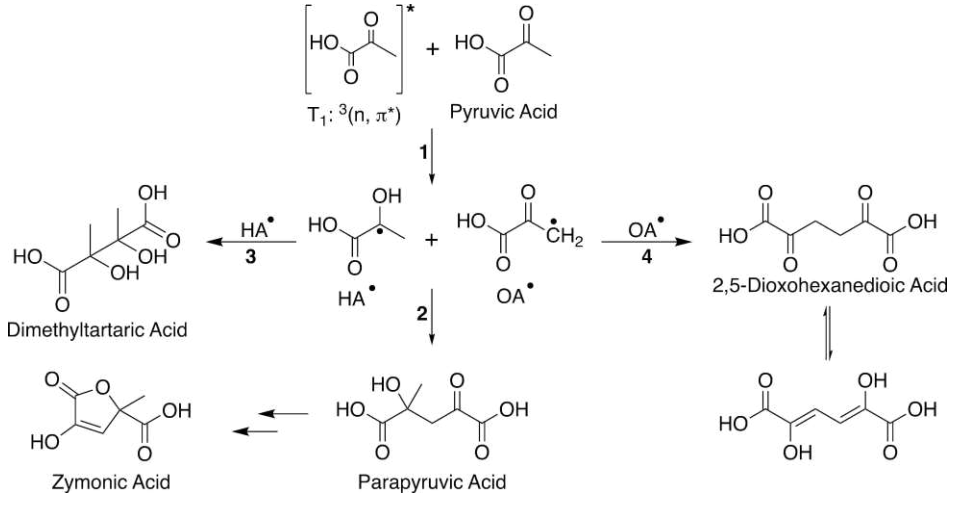

approximately 3.5, compared to ~2.4 for 10 mM solutions. At this lower concentration and higher pH, the amount of pyruvic acid in the keto conformer increases to about 75% (Supporting Information, Figure S4).

While all photochemical experiments were conducted under acidic conditions, the pH of the solutions are near the effective pK_a for pyruvic acid solutions of 2.49,[89] implying the protonation state of pyruvic acid is important to consider. This literature value is an effective pK_a because the keto and diol conformers have different, individual pK_a values, of 2.18 and 3.6, respectively.[82] Under our reaction conditions, then, more than 50% of the keto form of pyruvic acid is in its anionic form, pyruvate, for all concentrations, which reduces the number of photoactive protonated species in solution.

Regardless of the exact ratio of keto and diol conformer and their respective protonation states, the presence of significant amounts of protonated keto conformer in aqueous solution means that photochemistry is still a major reactive pathway under such conditions. However, interactions with the solvent shift the accessible electronic states for aqueous pyruvic acid, which favors photochemical mechanisms in the aqueous phase that follow different pathways than in the gas phase, as shown in Scheme 1.

In the aqueous phase, chemistry occurs from the T_1, $^3(n, \pi^*)$, state (reaction 1 in Scheme 1). As has been shown previously in the literature, the excited T_1 state can abstract a hydrogen from the carboxyl group of another pyruvic acid molecule and decarboxylates to form two radical species (reaction 2 in Scheme 1), one with hydroxyl acid functionality, $CH_3C(OH)CO_2H$, denoted as $HA^\bullet$ and one with geminal diol functionality, $CH_3C(OH)_2$, denoted as $GD^\bullet$.[37,43] The hydrogen abstraction from another pyruvic acid molecule can either occur from the keto form of the molecule or from its geminal diol form, 2,2-DHPA, though abstraction from the diol is favored energetically.[43] Because 10 mM pyruvic acid under our reaction conditions is approximately 50% in the diol form, it is likely that abstraction from the diol is the major pathway. It has also been suggested that proton-coupled electron transfer can also occur,[42,60] which would generate the same reactive radicals from the T_1 excited state of pyruvic acid.

The $HA^\bullet$ and $GD^\bullet$ radicals that are formed following hydrogen abstraction from the carboxyl group of either pyruvic acid or 2,2-DHPA, then go on to react further following a number of pathways, which are summarized in Scheme 1[37,43] with MS results given in Table 1. The branching ratio of the pathways, and therefore the yields of the generated species, is influenced by the environmental conditions under which the aqueous photochemistry is conducted. Under our reaction conditions, at 10 mM concentration under a nitrogen atmosphere, approximately 90% of the pyruvic acid is consumed during 5 h of irradiation (Supporting Information, Figure S3).

As is consistent with the previous literature, the main products observed from the aqueous phase photochemistry of pyruvic acid are oligomeric species, such as dimethyltartaric acid (DMTA), following reaction 4 of Scheme 1. DMTA is formed by the recombination of two $HA^\bullet$ radicals.[42,43] For this recombination to happen, the $HA^\bullet$ radicals must be able to escape from the initial solvent cage surrounding the generated $HA^\bullet$ and $GD^\bullet$ radicals in order to encounter a second $HA^\bullet$ radical. Because these radicals must both undergo cage escape and encounter one another in dilute solution to form dimethyltartaric acid, $HA^\bullet$ radicals must be relatively long-lived species. This observation is consistent with the stabilization of $HA^\bullet$ by the captodative effect, enabled by the presence of both electron-donating and electron-withdrawing groups.[90]

DMTA is not the only observed oligomeric product species. Previous ^1H NMR studies have observed a number of oligomeric photoproducts that remain unidentified.[37,43] Additionally, MS analyses consistently observe an oligomeric photoproduct ion that that is detected with similar intensity to DMTA and likely represents the chemical formula $C_7H_{12}O_5$.[37,42] The formation of this product cannot be explained following the mechanisms described in Scheme 1. It has been suggested previously that this species may be one of two possible structures, 2-(hydroxyethanyloxy)-2-carboxy-3ox-obutane or 2-(3-oxobutan-2-yloxy)-2-hydroxypropanoic acid.[42,70] Here, we propose that this product may be produced by further photochemistry of reactive oligomeric intermediates generated during photolysis with pyruvic acid.

The previously known mechanism for pyruvic acid aqueous photochemistry generates $HA^\bullet$ and $GD^\bullet$ following hydrogen abstraction from the carboxyl group of pyruvic acid or 2,2-DHPA.[43] Using electronic structure calculations, we examined the possibility of hydrogen abstraction from the methyl group

rather than the carboxyl group of a neutral pyruvic acid molecule, which, at the CBS-QB3 level, show that methyl hydrogen abstraction has a transition state that is 1.47 kcal/mol higher in enthalpy than that for abstraction from the carboxyl hydrogen. This is a small difference in energy that is close to the likely error in the method, suggesting that hydrogen abstraction from the methyl group is likely competitive with hydrogen abstraction from the carboxyl group of pyruvic acid. Abstraction from the methyl group may be further favored because, for all pyruvic acid concentrations under our reaction conditions, more than 50% of the keto form of pyruvic acid ($pK_a = 2.18$)[82] is in its anionic form, pyruvate. Photochemistry under high pH conditions (pH = 6.1), where most of the pyruvic acid is deprotonated, has been observed to be considerably slower than under more acidic conditions,[44] suggesting that hydrogen abstraction from the carboxyl group is indeed favored. However, for deprotonated pyruvate molecules only the methyl group is available for abstraction. While perhaps not the major location of abstraction, it is likely some abstraction from the methyl group of pyruvic acid occurs during the photochemical experiments (reaction 1 of Scheme 2),

yielding two radicals, $HA^{\bullet}$ and one with oxoacid functionality, $CH_2C(O)CO_2H$, denoted as $OA^{\bullet}$. It is worth noting that it is unlikely that proton-coupled electron transfer could generate the $OA^{\bullet}$ radical.

The recombination of $HA^{\bullet}$ and $OA^{\bullet}$ (reaction 2 of Scheme 2) generates parapyruvic acid, suggesting that it is a dimer of pyruvic acid that can be generated photochemically, in addition to dark oligomerization processes.[66] Each radical pair generated by hydrogen abstraction at the methyl group (Reaction 1 of Scheme 2) will have an overall net triplet characteristic, meaning that intracage geminate recombination to form parapyruvic acid will not occur. Instead, either intersystem crossing back to the singlet state or cage escape must take place before the radicals can react further, either of which is possible. The relative probability of these two possibilities, however, is difficult to predict.

If intersystem crossing back to the singlet state was the dominant pathway, one would expect only to see the recombination product between $HA^{\bullet}$ and $OA^{\bullet}$, generating parapyruvic acid. In the case of the radicals undergoing cage escape, the recombination product of each radical with itself would also be observed, in addition to the cross product between radicals. As is discussed above, the recombination of two $HA^{\bullet}$ radicals generates DMTA, which is shown in reaction 4 of Scheme 1 and in reaction 3 of Scheme 2. The recombination of two $OA^{\bullet}$ radicals would generate the dioxoacid compound shown by reaction 4 of Scheme 2. This dioxoacid, 2,5-dioxohexanedioic acid (DOHDA, $C_6H_6O_6$), would likely exist in equilibrium with its enol form, though we do not observe such a peak in the MS data. However, the absence of detection does not mean that this species is not formed. $OA^{\bullet}$, unlike $HA^{\bullet}$, is not stabilized by the captodative effect, so its lifetime would be expected to be somewhat shorter. It is also less likely to encounter another $OA^{\bullet}$ radical after undergoing cage escape because, while the energetics are not prohibitive, hydrogen abstraction from the methyl group of pyruvic acid is less likely than from the carboxyl group and thus $OA^{\bullet}$ concentrations are expected to be small. Additionally, the keto form of DOHDA will be in equilibrium with the enol form of the acid in aqueous solution. Both the keto and enol forms of DOHDA are likely to be themselves photoactive: the keto form has two α-keto acid groups and the enol form has a conjugated double bond system. This means that any DOHDA that might be generated during illumination may go on to react, further depleting its concentration in the post-irradiation solution and limiting our ability to detect it. It is possible that such reactions can account for some of the minor photoproducts that we currently have not identified.

Because we do not observe DOHDA in the MS data, we are unable to conclusively state whether intersystem crossing back to the singlet state or cage escape is the favored mechanistic pathway. We tentatively favor cage escape as the more likely path by which $HA^{\bullet}$ and $OA^{\bullet}$ may react with each other to form parapyruvic acid. Our reasons are 2-fold. First, because it provides another mechanistic pathway by which DMTA, a product observed in high concentrations, can be formed, and, second, because cage escape has been demonstrated to occur for both $HA^{\bullet}$ and $GD^{\bullet}$, as shown in Scheme 1.

Regardless of the path by which recombination of $HA^{\bullet}$ and $OA^{\bullet}$ occurs, it seems likely that parapyruvic acid is formed photochemically during the course of the illumination of pyruvic acid. This reactivity will reduce its concentration in solution and is likely the main reason it is not detected in the post-irradiation MS data with an intensity above the threshold we implement here. Parapyruvic acid, itself an α-keto acid, has the same reactive functionality as pyruvic acid, and is, therefore, capable of undergoing the same photochemistry as pyruvic acid, as shown in Scheme 3. Therefore, any trace parapyruvic acid in the initial pre-irradiation solution, as well as any generated photochemically, can also be excited by near-UV photons. An excited parapyruvic acid molecule may then abstract a hydrogen from either a pyruvic acid or 2,2-DHPA molecule, which would be followed by decarboxylation as in the pathway originally shown in reaction 2 of Scheme 1.

Scheme 3. Photochemistry of Parapyruvic Acid to Generate Trimer Species

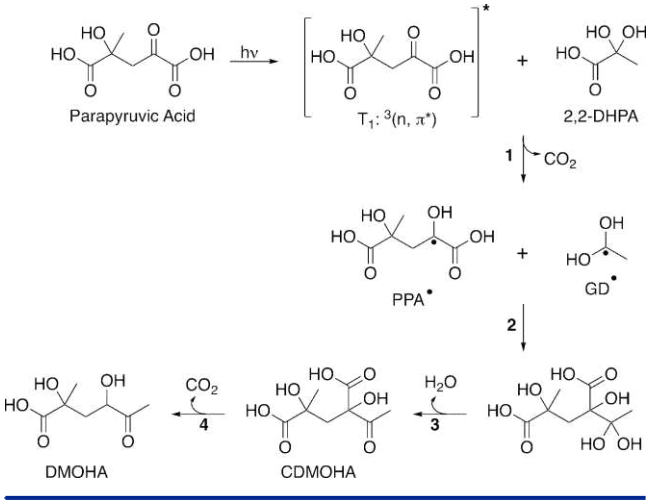

This generates both the familiar $GD^{\bullet}$ and a parapyruvic radical, $CO_2HC(CH_3)OHC(OH)CO_2H$ denoted as PPA, shown in reaction 1 of Scheme 3. These two radical species can then combine, following reactions 2 and 3 of Scheme 3, generating 4-carboxy-2,4-dihydroxy 2-methyl-5-oxohexanoic acid (CDMOHA) and, following decarboxylation (reaction 4 of Scheme 3), 2,4-dihydroxy-2-methyl-5-oxohexanoic acid (DMOHA). CDMOHA has a chemical formula of $C_8H_{12}O_7$ and we observe, correspondingly, a species in the MS data with an average experimental m/z for $[M-H]^-$ of 219.0517.

DMOHA's chemical formula is $C_7H_{12}O_5$. We posit that the oligomeric photoproduct that is detected in the MS data with a high intensity, both here and in the literature,[37,42] can be assigned to DMOHA and explained by the photochemical mechanism given in Scheme 3.

These structures, CDMOHA and DMOHA, are consistent with the MS results presented here and the known chemistry of pyruvic acid and zymonic acid.[37,43,66] The mechanistic pathway presented in Scheme 3 is further supported because it directly parallels one of the accepted mechanistic pathways for aqueous pyruvic acid photochemistry in the literature.[43,45] As shown by reaction 6 of Scheme 1, the recombination of the $HA^{\bullet}$ and $GD^{\bullet}$ radicals followed by the subsequent dehydration to form α-acetolactic acid, which then decarboxylates to form acetoin.[43] Consistent with this mechanism, we observe a species with an accurate mass corresponding to the chemical formula $C_5H_8O_4$, which is mostly likely acetolactic acid. Acetolactic acid, as a β-keto acid, will thermally decarboxylate into acetoin under ambient temperature conditions in aqueous solution. The rate of this decomposition is both pH and temperature dependent, increasing as temperature is raised and pH is lowered.[91] The time required for complete decarboxylation of aqueous acetolactic acid at 20 °C ranges from a few hours at a pH of 1.0[42] to 2 weeks at a pH of 4.65.[92] For our reaction conditions that are not buffered or pH adjusted (dependent on pyruvic acid concentration, pH ~ 2.4 for 10 mM pre-irradiation solutions), it is reasonable to expect that acetolactic acid generated photochemically would be partially decarboxylated, allowing us to observe both acetolactic acid and acetoin during post-irradiation analysis.

Acetoin has been widely reported in the literature as a known product of the aqueous photochemistry of pyruvic acid.[37,41,43−45] It is readily apparent that the pathway presented in Scheme 3 is wholly analogous to the pathway presented by reaction 6 of Scheme 1, where the intermediate species, CDMOHA, corresponds to acetolactic acid and DMOHA corresponds to acetoin. Griffith et al. unambiguously identified acetoin as a minor product by COSY NMR.[43] Here we identify acetoin as a photoproduct using ESI^- MS as well (Table 1).

The observation of acetoin as a product of the aqueous photochemistry of pyruvic acid has been a point of contention in the literature.[42,43,69,70] This discrepancy likely stems in part from the fact that acetoin is not a primary photoproduct, but, is instead formed from the thermal decarboxylation from a larger oligomer generated by radical−radical recombination. Indeed, several of the observed photoproducts of the light-initiated chemistry of pyruvic acid are not directly formed from the simple recombination of pyruvic acid-derived radicals. Rather, species that are generated by these initial recombination processes, such as 2-methyl-2,3,3-trihydroxybutanoic acid, go on to further react, forming species such as acetolactic acid and acetoin, as shown in Reaction 6 of Scheme 1. Such species can decompose into smaller product species, as is observed in the dehydration reactions that form acetolactic acid and CDMOHA and the decarboxylation reactions that form acetoin and DMOHA. But oligomeric intermediates can also react to generate larger oligomeric species, as is observed when parapyruvic acid, a dimer of pyruvic acid, is photochemically excited and reacts with another pyruvic acid molecule, ultimately generating DMOHA, a trimer of pyruvic acid. The generation and subsequent reactions of intermediate species, especially oligomeric intermediates, is not always appreciated. Because of this reactivity, both an increase in molecular complexity by the generation of oligomeric species and the generation of a complex mixture of molecules within the solution are observed. These interconnected reactions mean that even the three-carbon pyruvic acid generates a diverse library of products upon irradiation in aqueous solution. The combination of the reaction pathways outlined in Schemes 1−3, can explain the majority of the photochemical products observed in the MS data. This includes both acetic acid and lactic acid as shown in reaction 5 of Scheme 1. Acetic acid has been observed by NMR previously[43] and is readily seen in the NMR of the experiments conducted here (Supporting Information, Figures S3 and S4). Lactic acid was conclusively identified as a photoproduct by COSY and DOSY NMR.[43] Here, for the first time here we have observed the formation of lactic acid in the MS data as well (Table 1). However, there remain a number of minor photoproducts; we observe several that have not been previously reported in the literature and have not yet been identified. For completeness, we report the detailed MS data in Supporting Information, Table S1.

That the observed chemistry is so rich, even at very low pyruvic acid concentrations (from 0.5 to 10 mM), is perhaps surprising. We are able to detect more minor photoproducts in the 10 mM post-irradiation solutions in the MS, which is likely due to the lower concentration of products formed in solutions with lower initial pyruvic acid concentrations, as we used the same ionization parameters for all MS analyses. The main oligomeric products, including DMTA and DMOHA, are observed in the 0.5 mM post-irradiation solutions. The formation of these products requires that two radicals escape their initial solvent cage, encounter each other, and recombine before they are quenched. Even the initial generation of these radicals requires that a photoexcited species encounter another molecule in solution before quenching. Under more dilute conditions, the chance of such encounters occurring decreases. A kinetics analysis of the aqueous pyruvic acid photochemistry under anaerobic conditions found that the rates of depletion of pyruvic acid were roughly equivalent between 100 and 20 mM solutions,[37] suggesting that both of these concentrations are above this dilute limit. While a formal investigation of the kinetics of photolysis as a function of concentration was outside the scope of this study, the observed consumption of pyruvic acid in the NMR after 5 h of photolysis is lower for the low concentration solutions, as would be expected for radical-driven chemistry. For the solutions of 0.5 mM, the depletion of pyruvic acid was observed by NMR to be closer to 50% (Supporting Information, Figure S4), compared to the roughly 90% depletion observed for the 10 mM solutions. This observed decrease in reactivity is likely due to a combination of factors, all stemming from the low concentrations of pyruvic acid used. As mentioned above, in the 0.5 mM solutions, pyruvic acid exists primarily as the keto conformer and the higher pH of the solution (~3.5) means that more exists as pyruvate, both of which likely slow reaction compared to the 10 mM solutions. In the low concentration limit, it would also be expected that the probability of two species encountering each other before quenching decreases to essentially zero and only unimolecular homolysis products would be observed. It has previously been suggested that the transition from bimolecular to unimolecular processes would occur for solutions around 10 mM pyruvic acid.[42,60] Here, however, we demonstrate that under our reaction conditions bimolecular processes still readily occur even in very dilute solutions.

It is important to consider the implications of the reaction conditions used here, as the aqueous photochemistry of pyruvic acid is extremely sensitive to its environmental surroundings. This sensitivity helps explain differences between reported products in the literature.[37,41−45,69,70] As shown in Scheme 1, a number of pathways exist for the further reactions of $HA^{\bullet}$ and $GD^{\bullet}$ to give the observed photoproducts. The branching ratio of these pathways is influenced by the environmental conditions under which the aqueous photochemistry is conducted. For example, it has been shown that the composition of the atmosphere under which the photochemistry is conducted can strongly influence this branching ratio.[37] Reactions 3A and 3B of Scheme 1 involve the reaction of the radical species with oxygen. Reaction 3A is a pathway by which pyruvic acid is regenerated, therefore slowing the kinetics of pyruvic photolysis.[37] Reaction 3B forms acetic acid. In the high oxygen concentration limit, obtained by bubbling pure O_2 through the photolysis reactor, the branching ratio is such that only acetic acid is observed as a photoproduct using NMR (Supporting Information, Figure S5). Here, we are reliant on our combined, complementary NMR and ESI^- MS analyses: while acetic acid is formed and readily observed by NMR, it is not seen in the MS. Acetic acid is difficult to observe by the ESI^- MS used here, likely because, as a small molecule, it is toward the low mass range of our instrument, and the signal and mass accuracy of the instrument decrease as ion m/z is decreased. Even at 100 mM concentration, acetic acid is observed only weakly in the ESI^- MS, as shown in Supporting Information, Figure S6. It is not surprising that we do not observe it as a photoproduct in the MS when the concentration is much lower.

The effect to the branching ratio of the photochemical pathways under a pure O_2 atmosphere is extreme, but it serves as an example highlighting the differences in observable products created by different reaction conditions. In environments that are not saturated with O_2, the familiar oligomeric species discussed above are readily formed. In oxygen-limited conditions, these oligomers are the major observable products. Because we were interested primarily in these oligomeric species, we chose to conduct our photochemical experiments under a nitrogen atmosphere in order to maximize our ability to observe such species at low concentrations. Under conditions free of dissolved O_2, reaction 3 of Scheme 1 is effectively removed, and lifetimes of excited state pyruvic acid are effectively increased by removing the quenching effects of O_2. The oxygen-limited conditions may account for the persistence of bimolecular photochemical processes even at very dilute concentrations in the experiments reported here.

While the branching ratio observed for reactions under oxygen-depleted conditions is not directly comparable to those that might occur in the natural environment, the products observed and the mechanistic insight behind their formation provide us with a better understanding of the complexity of reactions that occur in the natural environment. Biasing the branching ratio toward oligomeric species for laboratory studies simply aids in the ability to analyze the resultant products at low concentrations, it does not change the nature of the species generated. Oxygen-limited conditions may additionally be relevant for certain systems found in the natural environment as well. Irradiation of pyruvic acid in the bulk aqueous phase open to air has been shown to deplete oxygen from the reaction vessel.[37,93] Atmospheric aerosols in the modern atmosphere are unlikely to be depleted in oxygen, but even under conditions

[37,61,93]

where dissolved O_2 is not depleted reactions to form oligomers are still active.

[95,99−101]

CONCLUSIONS

In this work, the aqueous phase photochemistry of pyruvic acid was investigated at low concentrations under an anaerobic, N_2 atmosphere. Even in very dilute solutions with low concen-trations of pyruvic acid, covalently bonded dimers and trimers are formed from the recombination of photochemically generated radical species. We have shown that it is energetically possible for an excited pyruvic acid molecule to abstract a hydrogen from the methyl hydrogen group of another pyruvic acid molecule in addition to hydrogen abstraction from the carboxyl group. This generates a new radical, $OA^{\bullet}$, which can recombine with $HA^{\bullet}$ to form parapyruvic acid, a dimer of pyruvic acid known to be generated via dark oligomerization processes.[66]

Several of the observed species in the post-irradiation solutions are not primary photoproducts of pyruvic acid but are, rather, generated from the further reactions of oligomeric intermediates. Such intermediate species can decompose by dehydration or decarboxylation, but they can also undergo further photochemical reactions to generate larger molecules. We have proposed that parapyruvic acid, itself an α-keto acid, when photoexcited follows the same photochemical pathways as pyruvic acid, cross-reacting with pyruvic acid to form 2,4-dihydroxy-2-methyl-5-oxohexanoic acid, a trimer of pyruvic acid.

Pyruvic acid's photochemistry is known to be incredibly sensitive to environmental conditions, with completely different reaction pathways available in the aqueous phase than in the gas phase. Within the aqueous phase, the composition of dissolved gases in solution has a strong influence on the branching ratio of these pathways. This network of reactions yields a diverse library of photoproducts even when considering only a simple model system of a single species. This highlights that the formation of SOA from the aqueous chemistry of small organics under atmospheric conditions is reliant on a Gordian Knot of interwoven networks of reactions between many species. However, while a complex mixture of products is generated from the aqueous photochemistry of pyruvic acid, the mechanisms governing their formation are robust and self-

consistent, suggesting that by understanding in detail the photochemistry of model species, mechanistic motifs may be found across classes of molecules that help untangle the reactive behavior of more complex mixtures of species.

ASSOCIATED CONTENT

* Supporting Information

The Supporting Information is available free of charge on the ACS Publications website at DOI: 10.1021/acs.jpca.7b03310.

Additional UV−vis, NMR, and high resolution ESI mass spectra, along with detailed tables of the mass spectrometry analysis and electronic structure calculation data (PDF)

AUTHOR INFORMATION

Corresponding Author

*(V.V.) E-mail: Vaida@colorado.edu.

ORCID

Veronica Vaida: 0000-0001-5863-8056

Notes

The authors declare no competing financial interest.

ACKNOWLEDGMENTS

We thank Allison E. Reed Harris and Jay A. Kroll for helpful discussions and feedback on the manuscript. We also thank Dr. Jeremy L. Balsbaugh and the University of Colorado at Boulder Central Analytical Laboratory Mass Spectrometry Core Facility (partially funded by NIH Grant S10 RR026641) for mass spectrometry measurements and advice about analysis. Financial support for R.J.R., R.J.P., and V.V. was provided by the National Science Foundation (CHE 1306386), the National Aeronautics and Space Administration under Grant No. NNX15AP20G issued through the Habitable Worlds Program, and a CIRES Innovative Research Proposal. R.J.P. acknowledges support from the NIH/CU Molecular Biophysics Training Program. R.J.R. also acknowledges support by NASA Headquarters under the NASA Earth and Space Science Fellowship Program, Grant NNX13AP85H, and partial support from both the University of Colorado Center for the Study of Origins and a CIRES Graduate Student Research Award.

REFERENCES

(1) Perraud, V.; Bruns, E. A.; Ezell, M. J.; Johnson, S. N.; Yu, Y.; Alexander, M. L.; Zelenyuk, A.; Imre, D.; Chang, W. L.; Dabdub, D.; et al. Nonequilibrium atmospheric secondary organic aerosol formation and growth. Proc. Natl. Acad. Sci. U. S. A. 2012, 109 (8), 2836−2841.

(2) Harrison, R. M.; Yin, J. Particulate matter in the atmosphere: Which particle properties are important for its effects on health? Sci. Total Environ. 2000, 249 (1), 85−101.

(3) Finlayson-Pitts, B. J.; Pitts, J. N. Chemistry of the upper and lower atmosphere; Academic Press: San Diego, CA, 1999.

(4) Hinds, W. C. Aerosol technology: Properties, behavior, and measurement of airborne particles, 2nd ed.; Wiley: New York, 1999.

(5) Ervens, B. Modeling the processing of aerosol and trace gases in clouds and fogs. Chem. Rev. 2015, 115 (10), 4157−4198.

(6) Lohmann, U.; Feichter, J. Global indirect aerosol effects: A review. Atmos. Chem. Phys. 2005, 5, 715−737.

(7) Hansen, J.; Sato, M.; Ruedy, R. Radiative forcing and climate response. J. Geophys. Res. Atmos. 1997, 102 (D6), 6831−6864.

(8) Hallquist, M.; Wenger, J. C.; Baltensperger, U.; Rudich, Y.; Simpson, D.; Claeys, M.; Dommen, J.; Donahue, N. M.; George, C.; Goldstein, A. H.; et al. The formation, properties and impact of secondary organic aerosol: Current and emerging issues. Atmos. Chem. Phys. 2009, 9 (14), 5155−5236.

(9) Ervens, B.; Turpin, B. J.; Weber, R. J. Secondary aerosol formation in cloud droplets and aqueous particles (aqsoa): A review of laboratory, field and model studies. Atmos. Chem. Phys. 2011, 11 (21), 11069−11102.

(10) Seinfeld, J. H.; Pandis, S. N. Atmospheric chemistry and physics: From air pollution to climate change; John Wiley & Sons, Inc.: New York, 1998.

(11) Boucher, O.; Randall, D.; Artaxo, P.; Bretherton, C.; Feingold, G.; Forster, P.; Kerminen, V. M.; Kondo, Y.; Liao, H.; Lohmann, U.; et al. Clouds and aerosols. In Climate change 2013: The physical science basis. Contribution of working group i to the fifth assessment report of the intergovernmental panel on climate change, Stocker, T. F., Qin, D., Plattner, G. K., Tignor, M., Allen, S. K., Boschung, J., Nauels, A., Xia, Y., Bex, V., Midgley, P. M., Eds. Cambridge Univ. Press: Cambridge, U.K., and New York, 2013; pp 465−570.

(12) Heald, C. L.; Jacob, D. J.; Park, R. J.; Russell, L. M.; Huebert, B. J.; Seinfeld, J. H.; Liao, H.; Weber, R. J. A large organic aerosol source in the free troposphere missing from current models. Geophys. Res. Lett. 2005, 32 (18), L18809.

(13) Jimenez, J. L.; Canagaratna, M. R.; Donahue, N. M.; Prevot, A. S. H.; Zhang, Q.; Kroll, J. H.; DeCarlo, P. F.; Allan, J. D.; Coe, H.; Ng, N. L.; et al. Evolution of organic aerosols in the atmosphere. Science 2009, 326 (5959), 1525−1529.

(14) Carlton, A. G.; Wiedinmyer, C.; Kroll, J. H. A review of secondary organic aerosol (soa) formation from isoprene. Atmos. Chem. Phys. 2009, 9 (14), 4987−5005.

(15) Monod, A.; Carlier, P. Impact of clouds on the tropospheric ozone budget: Direct effect of multiphase photochemistry of soluble organic compounds. Atmos. Environ. 1999, 33 (27), 4431−4446.

(16) Kroll, J. H.; Ng, N. L.; Murphy, S. M.; Flagan, R. C.; Seinfeld, J. H. Secondary organic aerosol formation from isoprene photooxidation. Environ. Sci. Technol. 2006, 40 (6), 1869−1877.

(17) Claeys, M.; Graham, B.; Vas, G.; Wang, W.; Vermeylen, R.; Pashynska, V.; Cafmeyer, J.; Guyon, P.; Andreae, M. O.; Artaxo, P. Formation of secondary organic aerosols through photooxidation of isoprene. Science 2004, 303 (5661), 1173−1176.

(18) Kroll, J. H.; Ng, N. L.; Murphy, S. M.; Flagan, R. C.; Seinfeld, J. H. Secondary organic aerosol formation from isoprene photooxidation under high - nox conditions. Geophys. Res. Lett. 2005, 32 (18), L18808.

(19) Bregonzio-Rozier, L.; Giorio, C.; Siekmann, F.; Pangui, E.; Morales, S.; Temime-Roussel, B.; Gratien, A.; Michoud, V.; Cazaunau, M.; DeWitt, H.; et al. Secondary organic aerosol formation from isoprene photooxidation during cloud condensation−evaporation cycles. Atmos. Chem. Phys. 2016, 16 (3), 1747−1760.

(20) George, C.; Ammann, M.; D'Anna, B.; Donaldson, D. J.; Nizkorodov, S. A. Heterogeneous photochemistry in the atmosphere. Chem. Rev. 2015, 115 (10), 4218−4258.

(21) Boris, A. J.; Desyaterik, Y.; Collett, J. L. How do components of real cloud water affect aqueous pyruvate oxidation? Atmos. Res. 2014, 143, 95−106.

(22) Vaida, V. Spectroscopy of photoreactive systems: Implications for atmospheric chemistry. J. Phys. Chem. A 2009, 113, 5−18.

(23) Altieri, K. E.; Carlton, A. G.; Lim, H.-J.; Turpin, B. J.; Seitzinger, S. P. Evidence for oligomer formation in clouds: Reactions of isoprene oxidation products. Environ. Sci. Technol. 2006, 40 (16), 4956−4960.

(24) Ervens, B.; Carlton, A. G.; Turpin, B. J.; Altieri, K. E.; Kreidenweis, S. M.; Feingold, G. Secondary organic aerosol yields from cloud-processing of isoprene oxidation products. Geophys. Res. Lett. 2008, 35 (2), L02816.

(25) Carlton, A. G.; Turpin, B. J.; Lim, H.-J.; Altieri, K. E.; Seitzinger, S. Link between isoprene and secondary organic aerosol (soa): Pyruvic acid oxidation yields low volatility organic acids in clouds. Geophys. Res. Lett. 2006, 33, L06822.

(26) Kawamura, K.; Kasukabe, H.; Barrie, L. A. Source and reaction pathways of dicarboxylic acids, ketoacids and dicarbonyls in arctic aerosols: One year of observations. Atmos. Environ. 1996, 30 (10−11), 1709−1722.

(27) Sempere, R.; Kawamura, K. Comparative distributions of dicarboxylic acids and related polar compounds in snow, rain, and aerosols from urban atmosphere. Atmos. Environ. 1994, 28 (3), 449− 459.
(28) Nguyen, T. B.; Bateman, A. P.; Bones, D. L.; Nizkorodov, S. A.; Laskin, J.; Laskin, A. High-resolution mass spectrometry analysis of secondary organic aerosol generated by ozonolysis of isoprene. Atmos. Environ. 2010, 44 (8), 1032−1042.
(29) Veres, P. R.; Roberts, J. M.; Cochran, A. K.; Gilman, J. B.; Kuster, W. C.; Holloway, J. S.; Graus, M.; Flynn, J.; Lefer, B.; Warneke, C.; et al. Evidence of rapid production of organic acids in an urban air mass. Geophys. Res. Lett. 2011, 38, L17807.
(30) Warneck, P. Multi-phase chemistry of c-2 and c-3 organic compounds in the marine atmosphere. J. Atmos. Chem. 2005, 51 (2), 119−159.
(31) Andreae, M. O.; Talbot, R. W.; Li, S. M. Atmospheric measurements of pyruvic and formic acid. J. Geophys. Res. 1987, 92 (D6), 6635−6641.
(32) Ho, K.; Lee, S.; Cao, J.; Kawamura, K.; Watanabe, T.; Cheng, Y.; Chow, J. C. Dicarboxylic acids, ketocarboxylic acids and dicarbonyls in the urban roadside area of hong kong. Atmos. Environ. 2006, 40 (17), 3030−3040.
(33) Talbot, R.; Andreae, M.; Berresheim, H.; Jacob, D. J.; Beecher, K. Sources and sinks of formic, acetic, and pyruvic acids over central amazonia: 2. Wet season. J. Geophys. Res. 1990, 95 (D10), 16799− 16811.
(34) Veres, P.; Roberts, J. M.; Burling, I. R.; Warneke, C.; de Gouw, J.; Yokelson, R. J. Measurements of gas - phase inorganic and organic acids from biomass fires by negative - ion proton - transfer chemical - ionization mass spectrometry. J. Geophys. Res. 2010, 115 (D23), D23302.
(35) Kawamura, K.; Kasukabe, H.; Barrie, L. A. Secondary formation of water-soluble organic acids and alpha-dicarbonyls and their contributions to total carbon and water-soluble organic carbon: Photochemical aging of organic aerosols in the arctic spring. J. Geophys. Res. 2010, 115, D21306.
(36) Mellouki, A.; Mu, Y. J. On the atmospheric degradation of pyruvic acid in the gas phase. J. Photochem. Photobiol., A 2003, 157 (2− 3), 295−300.
(37) Reed Harris, A. E.; Ervens, B.; Shoemaker, R. K.; Kroll, J. A.; Rapf, R. J.; Griffith, E. C.; Monod, A.; Vaida, V. Photochemical kinetics of pyruvic acid in aqueous solution. J. Phys. Chem. A 2014, 118 (37), 8505−8516.
(38) Lopalco, A.; Dalwadi, G.; Niu, S.; Schowen, R. L.; Douglas, J.; Stella, V. J. Mechanism of decarboxylation of pyruvic acid in the presence of hydrogen peroxide. J. Pharm. Sci. 2016, 105 (2), 705−713.
(39) Stefan, M. I.; Bolton, J. R. Reinvestigation of the acetone degradation mechanism in dilute aqueous solution by the uv/h2o2 process. Environ. Sci. Technol. 1999, 33 (6), 870−873.
(40) Schöne, L.; Herrmann, H. Kinetic measurements of the reactivity of hydrogen peroxide and ozone towards small atmospheri-cally relevant aldehydes, ketones and organic acids in aqueous solutions. Atmos. Chem. Phys. 2014, 14 (9), 4503.
(41) Leermakers, P. A.; Vesley, G. F. Photochemistry of alpha-keto acids and alpha-keto esters. 1. Photolysis of pyruvic acid and benzoylformic acid. J. Am. Chem. Soc. 1963, 85 (23), 3776−3779.
(42) Guzman, M. I.; Colussi, A. J.; Hoffmann, M. R. Photoinduced oligomerization of aqueous pyruvic acid. J. Phys. Chem. A 2006, 110 (10), 3619−3626.
(43) Griffith, E. C.; Carpenter, B. K.; Shoemaker, R. K.; Vaida, V. Photochemistry of aqueous pyruvic acid. Proc. Natl. Acad. Sci. U. S. A. 2013, 110 (29), 11714−11719.
(44) Leermakers, P. A.; Vesley, G. F. Photolysis of pyruvic acid in solution. J. Org. Chem. 1963, 28 (4), 1160−1161.
(45) Closs, G. L.; Miller, R. J. Photo-reduction and photo-decarbosylation of pyruvic acid - applications of cidnp to mechanistic photochemistry. J. Am. Chem. Soc. 1978, 100 (11), 3483−3494.
(46) Hall, G. E.; Muckerman, J. T.; Preses, J. M.; Weston, R. E.; Flynn, G. W. Time-resolved ftir studies of the photodissociation of pyruvic-acid at 193 nm. Chem. Phys. Lett. 1992, 193 (1−3), 77−83.
(47) Rincon, A. G.; Guzman, M. I.; Hoffmann, M. R.; Colussi, A. J. Optical absorptivity versus molecular composition of model organic aerosol matter. J. Phys. Chem. A 2009, 113 (39), 10512−10520.
(48) Vesley, G. F.; Leermakers, P. A. Photochemistry of alpha-keto acids and alpha-keto esters 0.3. Photolysis of pyruvic acid in vapor phase. J. Phys. Chem. 1964, 68 (8), 2364−2366.
(49) Dhanya, S.; Maity, D. K.; Upadhyaya, H. P.; Kumar, A.; Naik, P. D.; Saini, R. D. Dynamics of oh formation in photodissociation of pyruvic acid at 193 nm. J. Chem. Phys. 2003, 118 (22), 10093−10100.
(50) O'Neill, J. A.; Kreutz, T. G.; Flynn, G. W. Ir diode-laser study of vibrational-energy distribution in co2 produced by uv excimer laser photofragmentation of pyruvic-acid. J. Chem. Phys. 1987, 87 (8), 4598−4605.
(51) Wood, C. F.; O'Neill, J. A.; Flynn, G. W. Infrared diode-laser probes of photofragmentation products - bending excitation in co2 produced by excimer laser photolysis of pyruvic-acid. Chem. Phys. Lett. 1984, 109 (4), 317−323.
(52) Berges, M. G.; Warneck, P. Product quantum yields for the 350 nm photodecomposition of pyruvic acid in air. Ber. Bunsen-Ges. Phys. Chem. 1992, 96 (3), 413−416.
(53) Grosjean, D. Atmospheric reactions of pyruvic-acid. Atmos. Environ. 1983, 17 (11), 2379−2382.
(54) Yamamoto, S.; Back, R. A. The photolysis and thermal decomposition of pyruvic acid in the gas phase. Can. J. Chem. 1985, 63 (2), 549−554.
(55) Plath, K. L.; Takahashi, K.; Skodje, R. T.; Vaida, V. Fundamental and overtone vibrational spectra of gas-phase pyruvic acid. J. Phys. Chem. A 2009, 113, 7294−7303.
(56) Larsen, M. C.; Vaida, V. Near infrared photochemistry of pyruvic acid in aqueous solution. J. Phys. Chem. A 2012, 116, 5840− 5846.
(57) Takahashi, K.; Plath, K. L.; Skodje, R. T.; Vaida, V. Dynamics of vibrational overtone excited pyruvic acid in the gas phase: Line broadening through hydrogen-atom chattering. J. Phys. Chem. A 2008, 112 (32), 7321−7331.
(58) Reed Harris, A. E.; Doussin, J.-F.; Carpenter, B. K.; Vaida, V. Gas-phase photolysis of pyruvic acid: The effect of pressure on reaction rates and products. J. Phys. Chem. A 2016, 120 (51), 10123− 10133.
(59) Chang, X.-P.; Fang, Q.; Cui, G. Mechanistic photodecarboxylation of pyruvic acid: Excited-state proton transfer and three-state intersection. J. Chem. Phys. 2014, 141 (15), 154311.
(60) Davidson, R. S.; Goodwin, D.; De Violet, P. F. The mechanism of the photo-induced decarboxylation of pyruvic acid in solution. Chem. Phys. Lett. 1981, 78 (3), 471−474.
(61) Reed Harris, A. E.; Pajunoja, A.; Cazaunau, M.; Gratien, A.; Pangui, E.; Monod, A.; Griffith, E. C.; Virtanen, A.; Doussin, J. F.; Vaida, V. Multiphase photochemistry of pyruvic acid under atmospheric conditions. J. Phys. Chem. A 2017, 121, 3327−3339.
(62) Saito, K.; Sasaki, G.; Okada, K.; Tanaka, S. Unimolecular decomposition of pyruvic acid - an experimental and theoretical study. J. Phys. Chem. 1994, 98 (14), 3756−3761.
(63) Taylor, R. The mechanism of thermal eliminations xxiii: [1] the thermal-decomposition of pyruvic-acid. Int. J. Chem. Kinet. 1987, 19 (8), 709−713.
(64) da Silva, G. Decomposition of pyruvic acid on the ground-state potential energy surface. J. Phys. Chem. A 2016, 120 (2), 276−283.
(65) Colberg, M. R.; Watkins, R. J.; Krogh, O. D. Vibrationally excited carbon-dioxide produced by infrared multiphoton pyrolysis. J. Phys. Chem. 1984, 88 (13), 2817−2821.
(66) Perkins, R. J.; Shoemaker, R. K.; Carpenter, B. K.; Vaida, V. Chemical equilibria and kinetics in aqueous solutions of zymonic acid. J. Phys. Chem. A 2016, 120 (51), 10096−10107.
(67) Horowitz, A.; Meller, R.; Moortgat, G. K. The uv−vis absorption cross sections of the α-dicarbonyl compounds: Pyruvic

acid, biacetyl and glyoxal. J. Photochem. Photobiol., A 2001, 146 (1), 19−27.
(68) Schreiner, P. R.; Reisenauer, H. P.; Ley, D.; Gerbig, D.; Wu, C.-H.; Allen, W. D. Methylhydroxycarbene: Tunneling control of a chemical reaction. Science 2011, 332 (6035), 1300−1303.
(69) Griffith, E. C.; Carpenter, B. K.; Shoemaker, R. K.; Vaida, V. Reply to eugene et al.: Photochemistry of aqueous pyruvic acid. Proc. Natl. Acad. Sci. U. S. A. 2013, 110 (46), E4276−E4276.
(70) Eugene, A. J.; Xia, S.-S.; Guzman, M. I. Negative production of acetoin in the photochemistry of aqueous pyruvic acid. Proc. Natl. Acad. Sci. U. S. A. 2013, 110 (46), E4274−E4275.
(71) If not specified, the terms “dimer” and “trimer” are used here to refer to covalently bonded oligomeric species, rather than non-covalently associated species.
(72) Leermakers, P. A.; Vesley, G. F. Organic photochemistry and the excited state. J. Chem. Educ. 1964, 41 (10), 535.
(73) Turro, N. J.; Ramamurthy, V.; Scaiano, J. C. Modern molecular photochemistry of organic molecules; University Science Books: Sausalito, CA, 2010.
(74) Rossignol, S.; Tinel, L.; Bianco, A.; Passananti, M.; Brigante, M.; Donaldson, D. J.; George, C. Atmospheric photochemistry at a fatty acid−coated air-water interface. Science 2016, 353 (6300), 699−702.
(75) Montgomery, J. A.; Frisch, M. J.; Ochterski, J. W.; Petersson, G. A. A complete basis set model chemistry. Vi. Use of density functional geometries and frequencies. J. Chem. Phys. 1999, 110 (6), 2822−2827.
(76) Frisch, M. J.; Trucks, G. W.; Schlegel, H. B.; Scuseria, G. E.; Robb, M. A.; Cheeseman, J. R.; Scalmani, G.; Barone, V.; Petersson, G. A.; Nakatsuji, H.; et al. Gaussian 09, revision d.01; Gaussian, Inc.: Wallingford, CT, 2016.
(77) Ogg, R. J.; Kingsley, R.; Taylor, J. S. Wet, a t 1-and b 1-insensitive water-suppression method for in vivo localized 1 h nmr spectroscopy. J. Magn. Reson., Ser. B 1994, 104 (1), 1−10.
(78) Wolff, L. Ueber ein neues condensationsproduct der brenztraubensaure̋. Justus Liebigs Ann. Chem. 1901, 317 (1), 1−22.
(79) Prey, V.; Waldmann, E.; Berbalk, H. Zur kenntnis der brenztraubensaure̋. Monatsh. Chem. 1955, 86 (3), 408−413.
(80) Wolff, L. Ii. Ueber die parabrenztraubensaure̋. Justus Liebigs Ann. Chem. 1899, 305 (2), 154−165.
(81) Schnitzler, E. G.; Seifert, N. A.; Ghosh, S.; Thomas, J.; Xu, Y.; Jager̈, W. Hydration of the simplest α-keto acid: A rotational spectroscopic and ab initio study of the pyruvic acid−water complex. Phys. Chem. Chem. Phys. 2017, 19, 4440−4446.
(82) Pocker, Y.; Meany, J. E.; Nist, B. J.; Zadorojny, C. Reversible hydration of pyruvic acid. I. Equilibrium studies. J. Phys. Chem. 1969, 73 (9), 2879−2882.
(83) Buschmann, H. J.; Dutkiewicz, E.; Knoche, W. The reversible hydration of carbonyl compounds in aqueous solution.2. The kinetics of the keto gen-diol transition. Ber. Bunsen-Ges. Phys. Chem. 1982, 86, 129−134.
(84) Buschmann, H. J.; Fuldner, H. H.; Knoche, W. The reversible hydration of carbonyl compounds in aqueous solution. Part i, the keto/gem - diol equilibrium. Ber. Bunsen-Ges. Phys. Chem. 1980, 84 (1), 41−44.
(85) Vaida, V. Perspective: Water cluster mediated atmospheric chemistry. J. Chem. Phys. 2011, 135 (2), 020901.
(86) Kumar, M.; Francisco, J. S. The role of catalysis in alkanediol decomposition: Implications for general detection of alkanediols and their formation in the atmosphere. J. Phys. Chem. A 2015, 119 (38), 9821−9833.
(87) Kramer, Z. C.; Takahashi, H.; Vaida, V.; Skodje, R. T. Will water act as a photocatalyst for cluster phase chemical reactions? Vibrational overtone-induced dehydration reaction of methanediol. J. Chem. Phys. 2012, 136, 164302.
(88) Maroń, M. K.; Takahashi, K.; Shoemaker, R. K.; Vaida, V. Hydration of pyruvic acid to its geminal-diol, 2, 2-dihydroxypropanoic acid, in a water-restricted environment. Chem. Phys. Lett. 2011, 513 (4), 184−190.
(89) Pedersen, K. J. The dissociation constants of pyruvic and oxaloacetic acid. Acta Chem. Scand. 1952, 6 (2), 243−256.
(90) Viehe, H. G.; Janousek, Z.; Merenyi, R.; Stella, L. The captodative effect. Acc. Chem. Res. 1985, 18 (5), 148−154.
(91) Ronkainen, P.; Brummer, S.; Suomalainen, H.; et al. Diacetyl and formic acid as decomposition products of 2-acetolactic acid. Acta Chem. Scand. 1970, 24 (9), 3404−3406.
(92) De Man, J. The formation of diacetyl and acetoin from α -acetolactic acid. Recl. Trav. Chim. Pays-Bas 1959, 78 (7), 480−486.
(93) Renard, P.; Reed Harris, A. E.; Rapf, R. J.; Ravier, S.; Demelas, C.; Coulomb, B.; Quivet, E.; Vaida, V.; Monod, A. Aqueous phase oligomerization of methyl vinyl ketone by atmospheric radical reactions. J. Phys. Chem. C 2014, 118, 29421−29430.
(94) Ranjan, S.; Sasselov, D. D. Influence of the uv environment on the synthesis of prebiotic molecules. Astrobiology 2016, 16 (1), 68−88.
(95) Rapf, R. J.; Vaida, V. Sunlight as an energetic driver in the synthesis of molecules necessary for life. Phys. Chem. Chem. Phys. 2016, 18 (30), 20067−20084.
(96) Cooper, G.; Reed, C.; Nguyen, D.; Carter, M.; Wang, Y. Detection and formation scenario of citric acid, pyruvic acid, and other possible metabolism precursors in carbonaceous meteorites. Proc. Natl. Acad. Sci. U. S. A. 2011, 108 (34), 14015−14020.
(97) Voet, D.; Voet, J. G. Biochemistry, 4th ed.; John Wiley and Sons, Inc: Hoboken, NJ, 2011.
(98) Cody, G. D.; Boctor, N. Z.; Filley, T. R.; Hazen, R. M.; Scott, J. H.; Sharma, A.; Yoder, H. S. Primordial carbonylated iron-sulfur compounds and the synthesis of pyruvate. Science 2000, 289 (5483), 1337−1340.
(99) Griffith, E. C.; Shoemaker, R. K.; Vaida, V. Sunlight-initiated chemistry of aqueous pyruvic acid: Building complexity in the origin of life. Origins Life Evol. Biospheres 2013, 43, 341−352.
(100) Guzman, M. I.; Martin, S. T. Prebiotic metabolism: Production by mineral photoelectrochemistry of alpha-ketocarboxylic acids in the reductive tricarboxylic acid cycle. Astrobiology 2009, 9 (9), 833−842.
(101) Shapiro, R. Small molecule interactions were central to the origin of life. Q. Rev. Biol. 2006, 81 (2), 105−125.